1962-05

Higher-order geostrophic wind approximations

Arnason, G.

Monthly Weather Review, Vol. 90, No. 5, May 1962.
http://hdl.handle.net/10945/45639

DEPARTMENT OF COMMERCE
LUTHER H. HODGES, Secretary

WEATHER BUREAU
F. W. REICHELDERFER, Chief

MONTHLY WEATHER REVIEW

JAMES E. CASKEY, JR., Editor

Volume 90, Number 5 | Washington, D.C. | MAY 1962

HIGHER-ORDER GEOSTROPHIC WIND APPROXIMATIONS

G. 'ARNASON

Fleet Numerical Weather Facility, Monterey, Calif.

G. J. HALTINER

U.S. Naval Postgraduate School, Monterey, Calif.

and

LT. M. J. FRAWLEY

Fleet Numerical Weather Facility, Monterey, Calif.

[Manuscript received October 30, 1961; revised February 12, 1962]

ABSTRACT

Two iterative methods are described for obtaining horizontal winds from the pressure-height field by means of higher-order geostrophic approximations for the purpose of improving upon the geostrophic wind. The convergence properties of the iterative methods are discussed; and in a simple theoretical case, one of the methods is found to diverge with strong cyclonic motion. Both iterative methods were applied to analyzed 500-mb. height charts and over most of the map converged in a few scans to wind values somewhere between the geostrophic wind and the wind obtained from the balance equation. However in a few locations continued iteration led to increasing differences between successively computed winds; i.e., the methods appeared to diverge. In fact, wind values in adjacent areas gradually tended to be corrupted. This lack of convergence, occurring mainly in areas of negative vorticity and additionally in the case of method II in areas of strong cyclonic vorticity, was associated with the development of excessive horizontal wind divergence, which after three or four iterations sometimes exceeded the relative vorticity. Stream functions were computed by relaxing the relative vorticity of the winds obtained by methods I and II, generally after one iteration. These were compared to the stream function obtained by solving the balance equation and no significant differences were noted. Barotropic forecasts prepared from the stream functions derived from the two methods are essentially the same as forecasts with the stream function obtained from the balance equation.

1. INTRODUCTION

Few meteorological discoveries have been of more immediate and widespread use than the geostrophic wind law. Although exceedingly helpful in both practical and theoretical work, its obvious shortcomings have prompted a number of attempts at refinement by adding corrective terms consisting of higher order derivatives of pressure. In a remarkable paper on this subject in 1939, H. Philipps [1] expressed the horizontal wind, $\mathbf{V}$, as an infinite series in terms of the geostrophic wind, $\mathbf{V}_g$, and its total derivatives $d^n\mathbf{V}_g/dt^n$, where in the limit n approaches infinity. Although the series may converge for a properly restricted pressure distribution, it is of limited practical value because the total derivative contains the unknown wind, $\mathbf{V}$, itself. Thus if the series is truncated to a finite number of terms, m, the result is an algebraic equation for $\mathbf{V}$ of the mth order. It appears however from Philipps' study that a meaningful extension of the geostrophic wind law may be obtained by setting $n=1$, which amounts

to the same as replacing the acceleration term in the equation for horizontal motion by its geostrophic counterpart. Since the total derivative

$$\frac{d}{dt}=\frac{\partial}{\partial t}+\mathbf{V}\cdot\nabla+\omega\frac{\partial}{\partial p} \tag{1}$$

contains the wind $\mathbf{V}$, one may either replace $\mathbf{V}$ by $\mathbf{V}_g$ in (1) or retain it unaltered. The latter has been recommended by Eliassen [2] on the grounds that it, at least theoretically, leads to a better approximation. This point is treated at some length in section 2.

With the advent of electronic computers, wind calculations of the kind described above have become a possibility in routine operations and might from the point of view of time used be more economical to obtain than winds derived by solving the so-called balance equation. A relevant point, however, is whether the wind so computed is meteorologically more realistic than the geostrophic wind. Assuming this to be the case, the question of truncation and convergence of iterative procedures may have to be considered.

In a recent article, Endlich [3] proposed a method whereby a "gradient" wind is obtained by successive approximations. The method is appealing because of its simplicity in application and also because it appears in general to give winds that in the case of curved isobars are better than the geostrophic wind. A drawback, however, is that in areas of strong cyclonic curvature the iteration produces values for the wind that oscillate with undiminished or increased amplitude and will therefore never approach any fixed value; i.e., the procedure *diverges*.

One of the authors has elsewhere [4] studied theoretically the convergence properties of two iterative methods for solving the non-linear balance equation, one of which is in essence the same as the method proposed by Endlich. It was shown that the latter diverges in areas of strong cyclonic vorticity. This is further demonstrated in this paper by means of a simple theoretical case, as well as through computations from observed 500-mb. pressure heights. The other method was shown to converge in the case of non-divergent winds. This paper describes the application of similar methods to wind computations from 500-mb. heights. In this case no restrictions are imposed on the horizontal velocity divergence, and as a result both methods fail to give realistic winds in certain areas of the map. This failure manifests itself in the development of excessive vorticity and velocity divergence. By terminating the iterative procedure after one or two iterations, at least one of the methods appears to give winds that are everywhere better than the geostrophic winds. Winds derived by means of both methods were used as initial data to obtain stream functions from which 24- and 48-hour barotropic forecasts were made. The forecasts were essentially the same as those obtained through the use of the balance equation.

2. HIGHER-ORDER GEOSTROPHIC WIND APPROXIMATIONS

Omitting friction and the vertical advection terms[1] $\omega\partial u/\partial p$ and $\omega\partial v/\partial p$, we may write the equations for horizontal motion as follows:

$$\begin{aligned}\frac{\partial u}{\partial t}+u\frac{\partial u}{\partial x}+v\frac{\partial u}{\partial y}-fv+\frac{\partial\phi}{\partial x}&=0\\ \frac{\partial v}{\partial t}+u\frac{\partial v}{\partial x}+v\frac{\partial v}{\partial y}+fu+\frac{\partial\phi}{\partial y}&=0\end{aligned} \tag{2}$$

where the notations are those commonly used. It is desired to solve the system (2) with respect to u and v; i.e., express the wind as a function of the geopotential ϕ. A first approximation is the geostrophic relation

$$u_g=-\frac{1}{f}\frac{\partial\phi}{\partial y},\qquad v_g=\frac{1}{f}\frac{\partial\phi}{\partial x} \tag{3}$$

For motions on synoptic scale at middle and high latitudes, the approximation (3) is presumably accurate enough to apply also in differentiated form. This means that we may replace the derivatives of u and v in (2) by the corresponding derivatives of u_g and v_g and then solve the resulting equations for u and v. Thus we may obtain the following expressions for u and v:

$$\begin{aligned}u&=-\frac{1}{G}\left[\left(f-\frac{\partial u_g}{\partial y}\right)\left(\frac{\partial\phi}{\partial y}+\frac{\partial v_g}{\partial t}\right)+\frac{\partial v_g}{\partial y}\left(\frac{\partial\phi}{\partial x}+\frac{\partial u_g}{\partial t}\right)\right]\\ v&=\frac{1}{G}\left[\left(f+\frac{\partial v_g}{\partial x}\right)\left(\frac{\partial\phi}{\partial x}+\frac{\partial u_g}{\partial t}\right)-\frac{\partial u_g}{\partial x}\left(\frac{\partial\phi}{\partial y}+\frac{\partial v_g}{\partial t}\right)\right]\end{aligned} \tag{4}$$

where

$$G=\left(f-\frac{\partial u_g}{\partial y}\right)\left(f+\frac{\partial v_g}{\partial x}\right)+\frac{\partial u_g}{\partial x}\frac{\partial v_g}{\partial y}. \tag{5}$$

A necessary condition for (4) to be a solution to (2) is that $G\neq 0$. Since the system (2) is quadratic in u and v, there may be more than one solution for a given pressure distribution. The meteorologically appropriate solution for the wind should have essentially the same direction as the geostrophic wind and be identical with it in the case of straight, parallel isobars. Hence v should be of the same sign as $\partial\phi/\partial x$ and u of opposite sign to $\partial\phi/\partial y$, together with $G\neq 0$. It is not obvious how to achieve this in all cases, but one may be guided by the criteria applicable to the balance equation [4]. In solving this equation, the appropriate solution is obtained by requiring

$$\begin{aligned}f+2\frac{\partial v}{\partial x}&>0,\qquad f-2\frac{\partial u}{\partial y}>0\\ \left(f+2\frac{\partial v}{\partial x}\right)\left(f-2\frac{\partial u}{\partial y}\right)+4\frac{\partial u}{\partial x}\frac{\partial v}{\partial y}&>0\end{aligned} \tag{6}$$

and the additional restriction on the height field

[1] It is apparent that if several pressure levels were considered simultaneously, the vertical velocities could be computed diagnostically, and thus the terms $\omega\partial u/\partial p$ and $\omega\partial v/\partial p$ could be included.

$$\frac{1}{2}f^2+\nabla^2\phi-\nabla f\cdot\nabla\psi>0 \tag{7}$$

where ψ is the stream function. When the balance equation is linearized in the same way as the system (2), the criteria (6) are replaced by the weaker restrictions

$$f+\frac{\partial v}{\partial x}>0, \qquad f-\frac{\partial u}{\partial y}>0$$
$$\left(f+\frac{\partial v}{\partial x}\right)\left(f-\frac{\partial u}{\partial y}\right)+\frac{\partial u}{\partial x}\frac{\partial v}{\partial y}>0. \tag{6a}$$

This suggests that we impose the following limitations in solving (4):

$$f+\frac{\partial v_g}{\partial x}>0; \qquad f-\frac{\partial u_g}{\partial y}>0; \qquad G>0. \tag{6b}$$

Elimination of u_g and v_g from (5) by means of (3) gives the following expression for G:

$$G=f^2+\nabla^2\phi+f^{-2}(\phi_{xx}\phi_{yy}-\phi_{xy}^2)-f^{-1}\nabla f\cdot\nabla\phi$$
$$-f^3[f_x(\phi_x\phi_{yy}-\phi_y\phi_{xy})+f_y(\phi_y\phi_{xx}-\phi_x\phi_{xy})]>0 \tag{5a}$$

which resembles (7). A strict adherence to (6b) is somewhat cumbersome in practice and involves the solution of the non-linear differential inequality (5a). Rather than modify the pressure field in accordance with (6b), one may for practical reasons prefer to replace $f+(\partial v_g/\partial x)$, $f-(\partial u_g/\partial y)$, and G by suitable threshold values in the course of computing u and v from (4). This was done in the calculations reported on in this paper.

An inherent difficulty in applying (4) to height charts is the occurrence of time derivatives. Since initial height tendencies are not available, and height changes for the past 12 or 24 hours are of little value, one has little choice but to omit the time derivatives in the application of (4). Although this omission cannot be generally substantiated on theoretical grounds, there is some indirect empirical evidence (Rosenthal [5]) that at least at 500 mb. the time derivatives may be omitted. Rosenthal found that determinations of the 500-mb. geopotential field from observed winds by the use of the divergence equation corresponding to (2) (with time derivatives omitted) were quite accurate and as good, or slightly better, when the terms involving the space derivatives of velocity divergence were included. This suggests that winds obtained from (2) may be as useful as those obtained from the balance equation. We shall therefore ignore the time dependent terms with the reservation that such computed winds will be less accurate for pressure systems moving rapidly or in a stage of intense development. Thus (4) is reduced to

$$u=-\frac{1}{G}\left[\left(f-\frac{\partial u_g}{\partial y}\right)\frac{\partial\phi}{\partial y}+\frac{\partial v_g}{\partial y}\frac{\partial\phi}{\partial x}\right]$$
$$v=\frac{1}{G}\left[\left(f+\frac{\partial v}{\partial x}\right)\frac{\partial\phi}{\partial x}-\frac{\partial u_g}{\partial x}\frac{\partial\phi}{\partial y}\right] \tag{4a}$$

and should be solved subject to conditions (6b).

On the assumption that the wind derived from (4a) is better than the geostrophic wind, defined by (3), one can presumably iterate (4a) according to the scheme

$$u^{(n+1)}=-\frac{1}{G^{(n)}}\left[\left(f-\frac{\partial u^{(n)}}{\partial y}\right)\frac{\partial\phi}{\partial y}+\frac{\partial v^{(n)}}{\partial y}\frac{\partial\phi}{\partial x}\right]$$
$$v^{(n+1)}=\frac{1}{G^{(n)}}\left[\left(f+\frac{\partial v^{(n)}}{\partial x}\right)\frac{\partial\phi}{\partial x}-\frac{\partial u^{(n)}}{\partial x}\frac{\partial\phi}{\partial y}\right] \tag{4b}$$

with the restrictions

$$f-\frac{\partial u^{(n)}}{\partial y}>0; \qquad f+\frac{\partial v^{(n)}}{\partial x}>0;$$
$$G^{(n)}=\left(f-\frac{\partial u^{(n)}}{\partial y}\right)\left(f+\frac{\partial v^{(n)}}{\partial x}\right)+\frac{\partial u^{(n)}}{\partial x}\frac{\partial v^{(n)}}{\partial y}>0 \tag{6c}$$

in the expectation that $u^{(n+1)}$ and $v^{(n+1)}$ might converge to a stationary solution of (2). A similar procedure has been applied to the balance equation [4] and shown to converge subject to conditions analogous to (6); *i.e., stricter conditions than (6c)*. This would indicate that enforcement of (6c) would not always insure that the iterative scheme (4b) leads to a solution of (2) (omitting $\partial u/\partial t$ and $\partial v/\partial t$). If it converges at all, it may well lead to a solution intermediate between the geostrophic wind and a wind satisfying (2). Another possibility is that (4b) is semi-convergent in the sense that a few iterations will improve upon the geostrophic wind and that further iterations will either destroy the initial gain or not improve it any further. Actual computations indicate that this may be the case at least in some areas of the map.

Because of the difficulty in properly applying (6c) to the iterative scheme (4b), a simpler method will be discussed briefly. This method consists in omitting $\partial u/\partial t$ and $\partial v/\partial t$ in (2) as before, but replacing the remaining acceleration terms entirely by their geostrophic counterparts, and then solving with respect to u and v. If repeated, this procedure leads to the iterative scheme

$$u^{(n+1)}=u_g-\frac{u^{(n)}}{f}\frac{\partial v^{(n)}}{\partial x}-\frac{v^{(n)}}{f}\frac{\partial v^{(n)}}{\partial y}$$
$$v^{(n+1)}=v_g+\frac{u^{(n)}}{f}\frac{\partial u^{(n)}}{\partial x}+\frac{v^{(n)}}{f}\frac{\partial u^{(n)}}{\partial y}. \tag{8}$$

In this case no apparent restrictions need to be imposed on the pressure field. A scheme similar to (8) was discussed by Endlich [3] who proposed its use for routine operations as a replacement for the geostrophic wind and the wind derived by the balance equation. The iterative scheme (8) has been applied to the solution of the balance equation and shown to diverge under certain conditions [4].

In order to illustrate the difference between (8) and (4b) and the condition under which (8) does not converge, we shall apply both schemes to the gradient wind equation

$$\frac{v^2}{r}+fv=fv_g \tag{9}$$

TABLE 1.—*Shown here are the results of successive iterations of methods I and II applied to the gradient wind equation for several cases of stationary cyclonic and anticyclonic motion*

	Cyclonic Motion						Anticyclonic Motion					
	$v_g=0.5\,fr$		$v_g=1.0\,fr$		$v_g=1.5\,fr$		$v_g=-\frac{1}{16}fr$		$v_g=-\frac{1}{8}fr$		$v_g=-\frac{1}{4}fr$	
n	I	II	I	II	I	II	I	II	I	II	I	II
1	$0.667v_g$	$0.500v_g$	$0.500v_g$	$0.000v_g$	$0.400v_g$	$-0.500v_g$	$1.067v_g$	$1.063v_g$	$1.140v_g$	$1.130v_g$	$1.333v_g$	$1.250v_g$
2	$0.750v_g$	$0.875v_g$	$0.667v_g$	$1.000v_g$	$0.625v_g$	$+0.625v_g$	$1.071v_g$	$1.071v_g$	$1.166v_g$	$1.158v_g$	$1.500v_g$	$1.391v_g$
3	$0.727v_g$	$0.609v_g$	$0.600v_g$	$0.000v_g$	$0.516v_g$	$+0.414v_g$	$1.072v_g$	$1.172v_g$	$1.170v_g$	$1.167v_g$	$1.600v_g$	$1.483v_g$
4	$0.733v_g$	$0.810v_g$	$0.625v_g$	$1.000v_g$	$0.564v_g$	$+0.743v_g$			$1.171v_g$	$1.170v_g$	$1.677v_g$	$1.550v_g$
5	$0.732v_g$	$0.672v_g$	$0.615v_g$	$0.000v_g$	$0.542v_g$	$+0.172v_g$			$1.172v_g$	$1.171v_g$	$1.715v_g$	$1.601v_g$
6		$0.774v_g$	$0.619v_g$	$1.000v_g$	$0.552v_g$	$+0.956v_g$				$1.171v_g$	$1.750v_g$	$1.641v_g$
7		$0.701v_g$	$0.618v_g$		$0.547v_g$	$-0.369v_g$				$1.172v_g$	$1.778v_g$	$1.673v_g$
8		$0.754v_g$			$0.549v_g$	$+0.795v_g$					$1.800v_g$	$1.700v_g$
9		$0.715v_g$				$+0.051v_g$					$1.818v_g$	$1.722v_g$
10		$0.743v_g$				$+0.996v_g$					$1.833v_g$	$1.741v_g$
11		$0.723v_g$		Oscillation		$-0.488v_g$					$1.846v_g$	$1.758v_g$
12		$0.738v_g$				$+0.642v_g$					$1.857v_g$	$1.773v_g$
13		$0.728v_g$				$+0.381v_g$					$1.867v_g$	$1.786v_g$
14		$0.735v_g$				$+0.782v_g$					$1.875v_g$	$1.797v_g$
15		$0.730v_g$				$+0.082v_g$					$1.882v_g$	$1.807v_g$
16		$0.734v_g$				$+0.989v_g$					$1.889v_g$	$1.817v_g$
17		$0.731v_g$				$-0.470v_g$					$1.895v_g$	$1.825v_g$
v	$0.732\,v_g$		$0.618\,v_g$		$0.549\,v_g$		$1.072\,v_g$		$1.172\,v_g$		$2.00\,v_g$	

where r is the radius of curvature, positive for cyclonic motion and negative for anticyclonic motion; v is the wind speed, and v_g, its geostrophic counterpart. Equation (9) has the two solutions

$$v=\frac{fr}{2}\left(-1\pm\sqrt{1+\frac{4v_g}{fr}}\right). \tag{9a}$$

In the cyclonic case, $r>0$, the plus sign applies; when $r<0$, both solutions give rotation in the same sense around the high pressure center. The negative sign corresponds to the so-called anomalous solution discussed elsewhere [6]. It can be seen directly from (9a) that the plus sign corresponds to $f+2(v/r)>0$ and the minus sign to $f+2(v/r)<0$. The condition for a real solution of (9) is

$$\frac{1}{4}f+\frac{v_g}{r}\geq 0 \tag{10}$$

which leads to the additional restriction for the normal solution; i.e., the one corresponding to the plus sign,

$$v\leq 2v_g. \tag{10a}$$

In applying the iterative schemes (4b), denoted I below, and (8), denoted II, we shall distinguish between anticyclonic and cyclonic motion; and in the cyclonic case further distinguish between (a) $v_g<fr$, and (b) $v_g\geq fr$. The solution of (9a) with which we compare is the normal solution. Table 1 shows the results of the computations. Apparently method I approaches the true solution in all cases, although very slowly for the limiting case $v_g=-\frac{1}{4}fr$. The convergence of method II is slower and it diverges in the case of cyclonic motion when $v_g\geq fr$, as predicted by theory [4]. Note the vacillating amplitude of the error of method II when $v_g\geq fr$; this is further illustrated in figure 1. In Endlich's article [3], method II is shown to converge in the two cases selected. These turn out to correspond to $v_g=5fr/16$ and $v_g=-5fr/36$, respectively.

The following section describes the application of both methods to 500-mb. heights from analyzed maps.

3. RESULTS OF WIND AND VORTICITY COMPUTATIONS FROM ANALYZED HEIGHT MAPS

The iterative schemes (4b) and (8), denoted methods I and II respectively, were applied to analyzed 500-mb. height charts. In applying method I, the following restrictions were imposed in accordance with (6c):

(a) an arbitrary lower limit of 0.25 was imposed on the terms $\left(1+\frac{1}{f}\frac{\partial v^{(n)}}{\partial x}\right)$ and $\left(1-\frac{1}{f}\frac{\partial u^{(n)}}{\partial y}\right)$

(b) the quantity $G^{(n)}/f^2$ was not allowed to become smaller than 0.125.

As it turned out both methods gave essentially the same results over most of the map and converged within a few scans to a certain wind value in much the same way as in the case of the gradient wind treated in the previous section. In certain spots, however, both methods showed lack of convergence in that the difference between successive iterations either increased with the number of iterations or oscillated undiminished. With an increased number of iterations, these initially small "trouble spots" would expand and ultimately corrupt the winds elsewhere. This lack of convergence was closely associated with the development of pronounced horizontal wind divergence which after three or four iterations might equal or surpass the relative vorticity. In retrospect this is not so surprising since neither method has any inherent controls on the horizontal velocity divergence. This lack of control would seem to explain why method I shows instability as applied here, although it is stable when applied to the balance equation; *i.e., in deriving non-divergent winds.* Attempts to restrict somewhat arbitrarily the magnitude of the velocity divergence in the course of the iterations did to some extent suppress

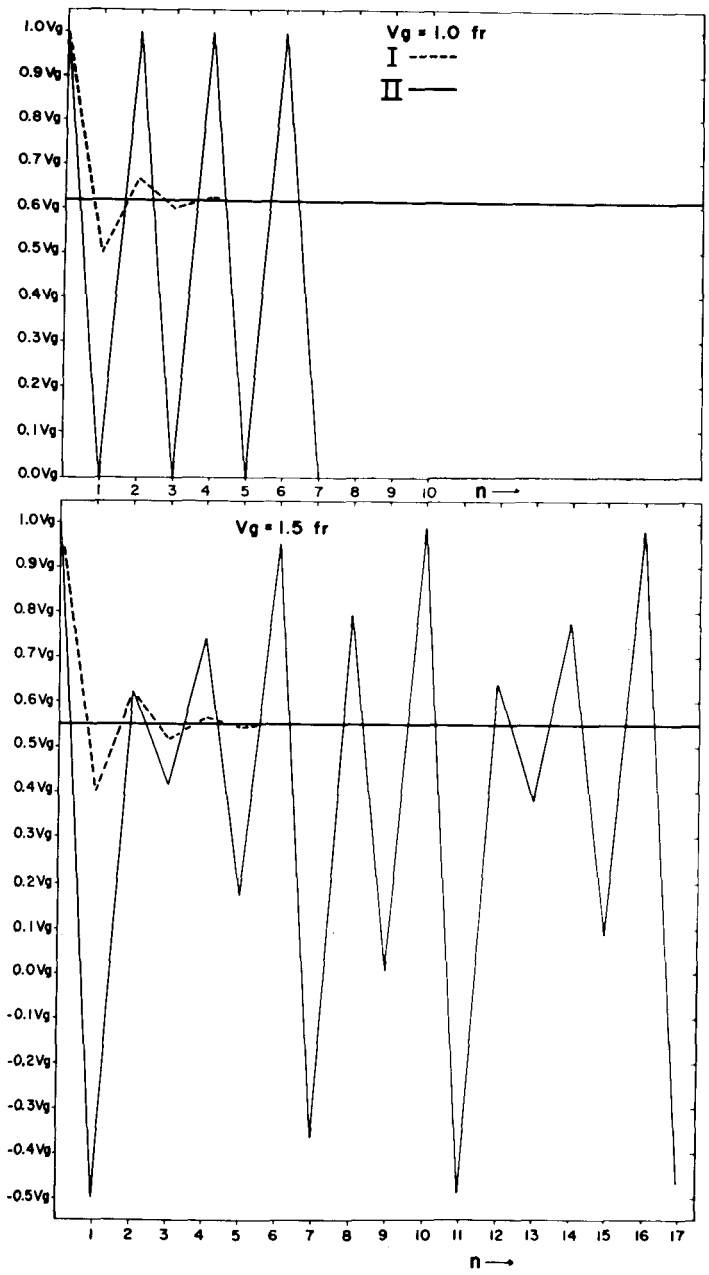

FIGURE 1.—Graph showing successive approximations to the gradient wind speed (horizontal line) for cyclonic motion (v_g expressed in terms of fr). Dashed lines join approximations computed by method I; solid lines join approximations computed by method II.

the instability of both methods but did not eliminate it. This instability was also reduced by ellipticizing the height field by imposing (7).

Some of the results are summarized in tables 2–5. Table 5 displays the difference between the two methods in the case of large cyclonic vorticities. As predicted by theory [4], method II appears to diverge in points where the ratio ζ_g/f exceeds unity. The locations of the selected points A, B, C, D, E are shown on the geostrophic vorticity map, figure 3. Figure 2 shows the areas where method I displays instability in relation to the pressure pattern. These areas do not occur at high latitudes and are predominantly associated with negative relative vorticities. Outside the dashed areas, the difference $V_3 - V_2$ is less than 3 m. sec.$^{-1}$ and mostly less than 1 m. sec.$^{-1}$ It is apparent from tables 2–4 that in areas of marked cyclonic curvature both methods result in sub-geostrophic wind speeds; the reverse holds true in areas of anticyclonic curvature.

When wind values obtained from successive iterations oscillate, obviously it would be advantageous to reduce the oscillation. This can be accomplished either by averaging wind values obtained from two successive iterations and utilizing these averages for evaluating the velocity derivatives in the next iteration; or by deliberately "under-relaxing"; i.e., applying only a fraction of the correction due to the acceleration terms to the geostrophic wind. If the latter method is employed such "under-relaxation" coefficients clearly must be chosen to approach unity in successive iterations. Similarly, in regions where the wind values obtained from successive iterations monotonically approach a limit, a series of "over-relaxation" coefficients progressively approaching unity could be used

TABLE 2.—*Maximum difference between computed and geostrophic wind speeds observed in selected areas of well-defined cyclonic curvature*

Location	Geostrophic wind speed	Method I		Method II	
		$\lvert V_1\rvert-\lvert V_g\rvert$	$\lvert V_2\rvert-\lvert V_g\rvert$	$\lvert V_1\rvert-\lvert V_g\rvert$	$\lvert V_2\rvert-\lvert V_g\rvert$
	(*m.p.s.*)	(*m.p.s.*)	(*m.p.s.*)	(*m.p.s.*)	(*m.p.s.*)
Eastern United States	50–58	−17	−14	−26	−8
Eastern Atlantic	30–38	−12	−9	−19	−5
Eastern Europe	30–38	−8	−6	−11	−4
Off East Coast of Asia	50–62	−20	−12	−31	−2
Central Pacific	50–60	−19	−13	−28	−7

TABLE 3.—*Maximum difference between computed and geostrophic wind speeds observed in selected areas of well-defined anticyclonic curvature*

Location	Geostrophic wind speed	Method I		Method II	
		$\lvert V_1\rvert-\lvert V_g\rvert$	$\lvert V_2\rvert-\lvert V_g\rvert$	$\lvert V_1\rvert-\lvert V_g\rvert$	$\lvert V_2\rvert-\lvert V_g\rvert$
	(*m.p.s.*)	(*m.p.s.*)	(*m.p.s.*)	(*m.p.s.*)	(*m.p.s.*)
Off East Coast of North America	15–20	+13	+9	+7	+9
Siberia	25–31	+8	+8	+6	+7
Central Pacific	30–39	+18	+8	+11	+12
Western Canada	4–14	+3	+2	+2	+2

TABLE 4.—*Maximum value of center of cyclonic relative vorticity; unit 10^{-6} sec.$^{-1}$*

Position of associated Low	ζ_g	Maximum value of center of cyclonic relative vorticity					
		Method I			Method II		
		ζ_1	ζ_2	ζ_3	ζ_1	ζ_2	ζ_3
39° N., 10° E.	67	52	56	54	47	60	59
58° N., 22° E.	85	68	72	71	63	70	69
38.5° N., 33° E.	80	63	68	67	58	73	63
78.5° N., 88° E.	38	34	34	34	34	36	34
54° N., 147° E.	75	61	63	63	57	65	62
56° N., 164° W.	59	51	52	52	50	51	52
84° N., 135° W.	57	51	52	52	50	52	52
55° N., 71° W.	91	75	79	79	71	74	77
46° N., 23° W.	99	68	83	76	59	92	67

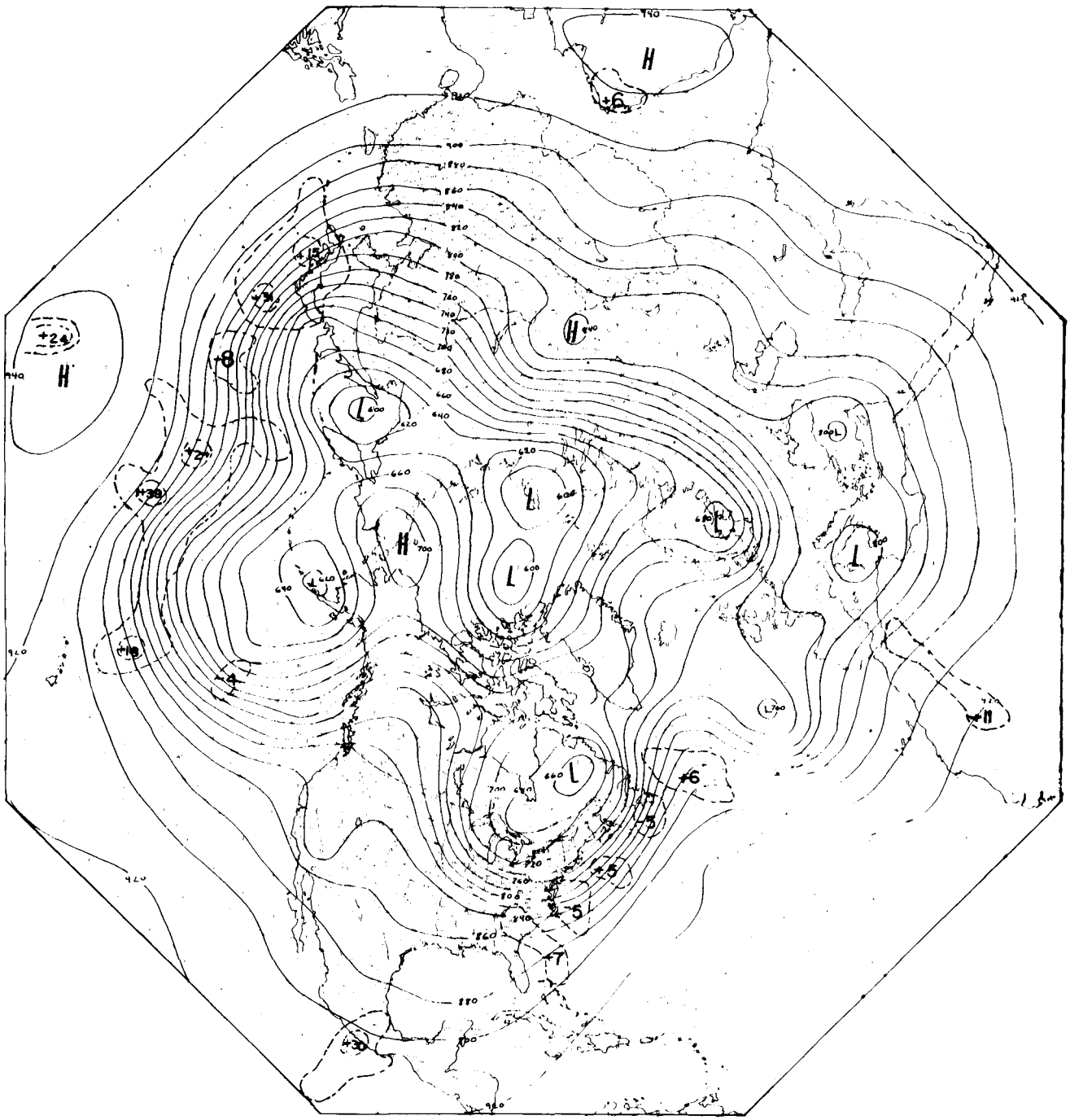

FIGURE 2.—January 3, 1958, 0000 GMT. 500-mb. contours (solid) with velocity differences (dashed) between second and third iterations ($V_3 - V_2$), as computed by method I. Outside instability areas, velocity differences are less than 3 m. sec.$^{-1}$

TABLE 5.—*Successive vorticities computed by methods I and II for cases of high ζ_g/f ratios*

	$\frac{\zeta_g}{f}$	Method I				Method II			
		ζ_g	ζ_1	ζ_2	ζ_3	ζ_g	ζ_1	ζ_2	ζ_3
A	1.14	105	67	95	97	105	42	122	20
B	1.33	127	86	113	100	127	64	144	50
C	0.95	98	71	78	76	98	59	88	67
D	0.99	98	66	78	72	98	50	92	56
E	1.04	99	68	83	76	99	54	97	58

to expedite convergence. Such methods were applied and generally accomplished the desired results. However in the previous trouble spots, though the oscillations were initially reduced, they were not entirely eliminated; and both iterative methods eventually diverged in these areas.

The relative vorticity of winds derived by the above discussed methods after 1–2 iterations is approximately the same as derived by means of the balance equation. Both methods, however, give non-zero velocity divergence; and it is of interest to know whether this has any synoptic significance. In an attempt to judge this, method I was

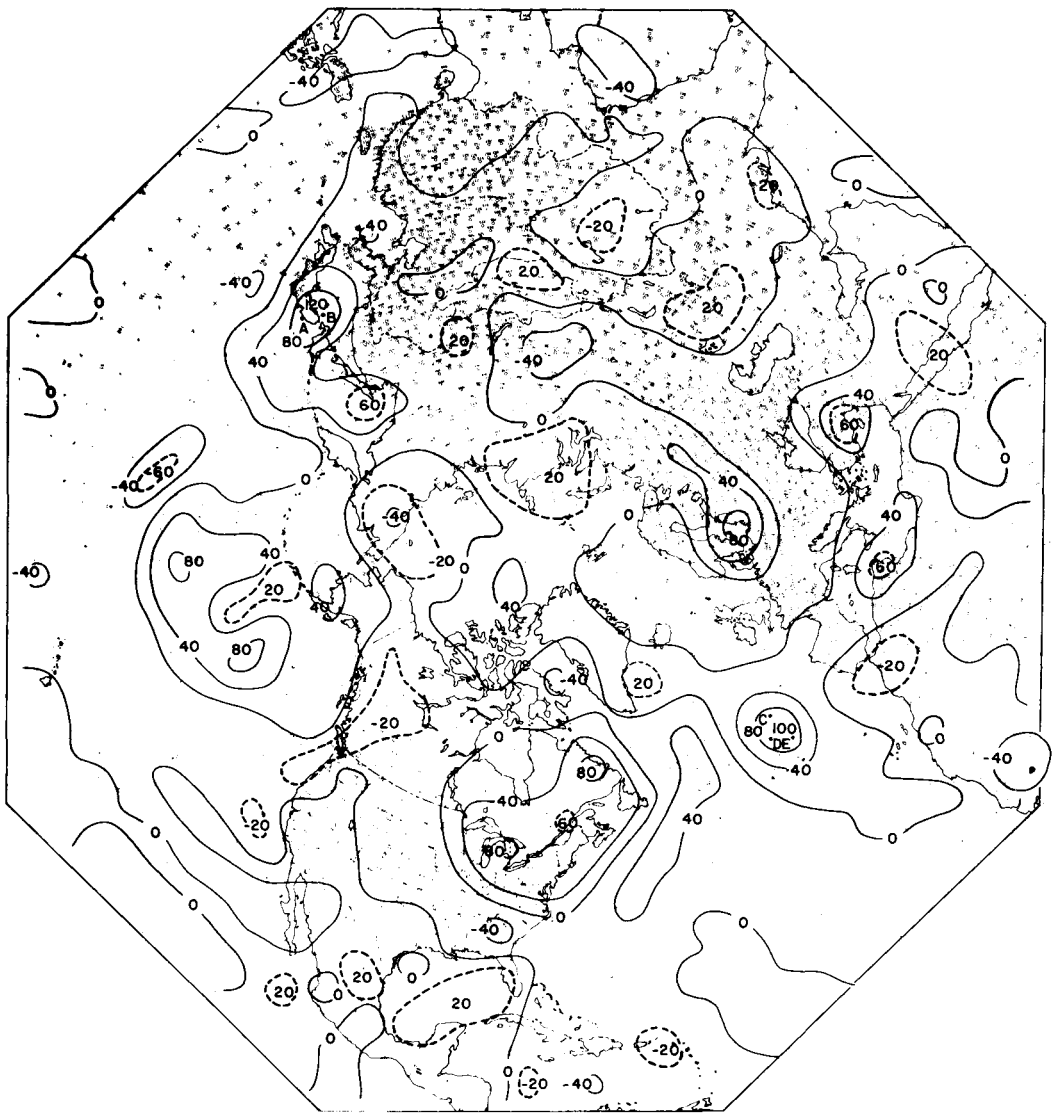

FIGURE 3.—The field of geostrophic relative vorticity in units of 10^{-6} sec.$^{-1}$, January 3, 1958, 0000 GMT. A, B, C, . . . , correspond to points for which the computations of table 5 were made.

applied to an 850-mb. chart and the horizontal wind divergence formed; the latter was also computed by means of a simple prediction model [7]. These results are in figures 4 and 5 superposed upon the 850-mb. height contours; obviously they differ greatly. Since the velocity divergence derived by means of the prediction model could account for the observed displacement of the major pressure systems, it is tentatively concluded that the divergence obtained by method I, shown in figure 4, is essentially a noise phenomenon. It should also be mentioned that the velocity divergence computed by either method did not change appreciably with succeeding iterations, except in the small instability areas mentioned above.

4. BAROTROPIC FORECASTS USING HIGHER-ORDER GEOSTROPHIC WIND APPROXIMATIONS

Stream functions corresponding to the relative vorticities obtained by methods I and II are easily obtained by solving the Poisson equation[2] $\zeta=(g/\bar{f})\nabla^2\psi$ using the relaxation technique. This equation was in most cases solved for $n=1$ only, i.e., one iteration; and the following discussion is confined to this case alone except when stated otherwise. A comparison of the computed stream function fields with those obtained by solving the balance equation reveals that, in all instances, the gradient of ψ between the North Pole and the octagonal grid boundaries for the fields computed by the methods of this study is slightly greater than those computed through the balance equation. In the cases studied the difference varied from 200 to 400 feet. This means that the non-divergent parts of the winds computed by the methods described herein slightly exceed those obtained through the balance equation. Since the difference in the stream function gradient is almost uniform from the North Pole to the boundaries, the difference in wind speed at any point is only of the order of centimeters per second.

[2] ψ so defined has the dimension of length; the corresponding wind is $\mathbf{V}=(g/\bar{f})\mathbf{k}\times\nabla\psi$.

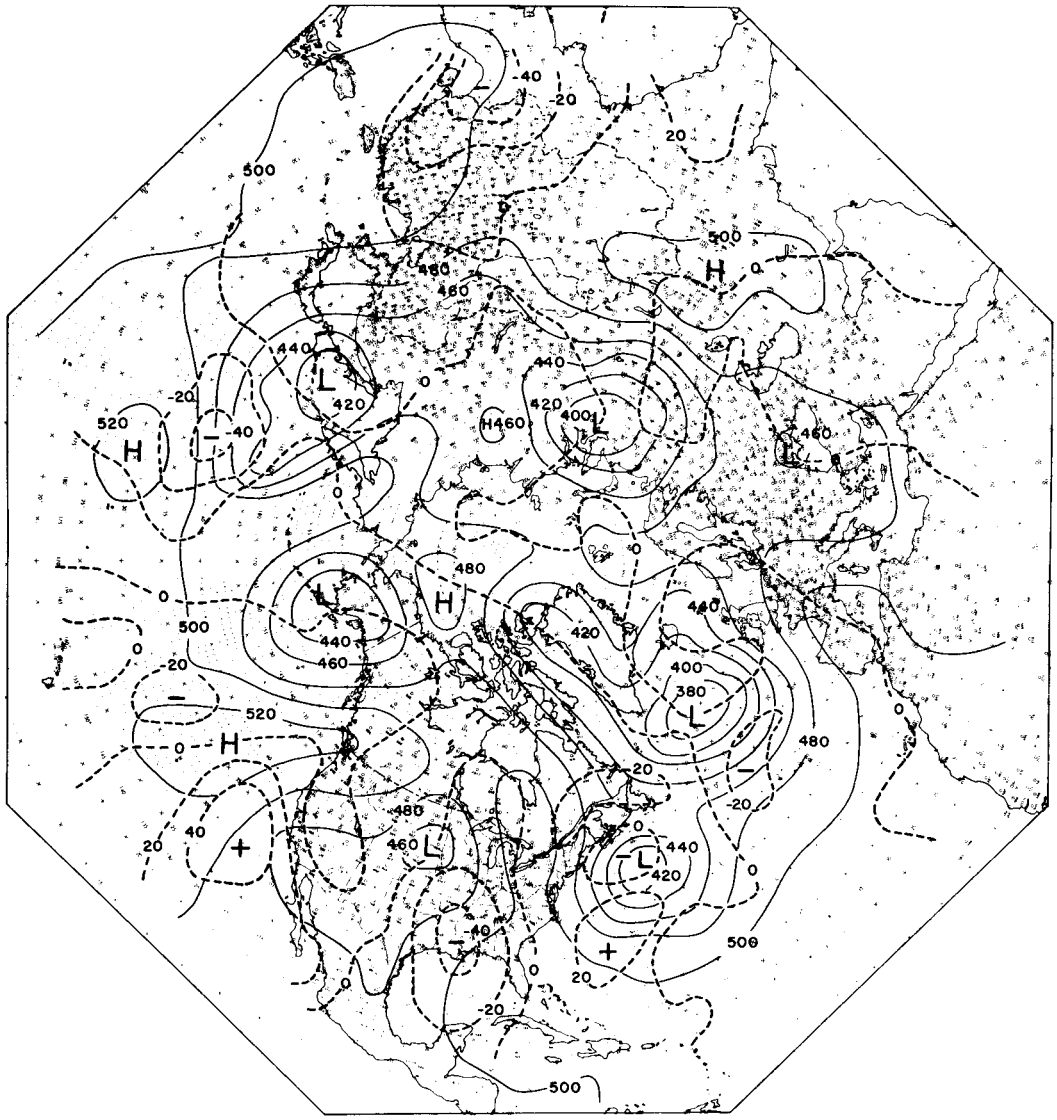

FIGURE 4.—0300 GMT, April 5, 1955. 850-mb. contours (solid) with the horizontal velocity divergence obtained by method I superimposed (dashed lines). Units 10^{-7} sec.$^{-1}$

An examination of the stream fields obtained by method I reveals that the decrease in the amplitude of major height troughs is slightly greater than that obtained by means of the balance equation. This decrease in amplitude is more pronounced in the ψ-fields computed by means of method II, presumably because of the underestimation of the wind by this method as previously mentioned. As the number of iterations increases this weakening of troughs decreases, the amplitude of the features being approximately the same as those of the ψ-fields of the balance equation.

In order to investigate the feasibility of using the stream functions derived by means of methods I and II as initial fields for forecasts, a few 24- and 48-hour prognoses were made using the barotropic vorticity equation

$$\nabla^2\frac{\partial\psi}{\partial t}+\mathbf{J}(\psi,\eta)-\frac{\mu\eta}{\bar{\psi}}\frac{\partial\psi}{\partial t}=0 \tag{11}$$

where $\mathbf{J}$ is the Jacobian operator [8]. The term $-(\mu\eta/\bar{\psi})\,\partial\psi/\partial t$ is added to the vorticity equation for non-divergent flow in order to stabilize the planetary waves. In these computations μ was assigned the value 4, in accordance with the results derived by Cressman [9]. For the sake of comparison, forecasts were also made by means of the stream function obtained through the balance equation. For verification purposes, difference fields were formed and a "pillow" and a root-mean-square error were computed over the entire grid using the formulae

$$\text{Pillow}=\frac{\sum_{n=1}^{1977}(A-B)_n}{1977} \tag{12}$$

$$\text{RMSE}=\sqrt{\frac{\sum_{n=1}^{1977}[(A-B)-\text{Pillow}]_n^2}{1977}} \tag{13}$$

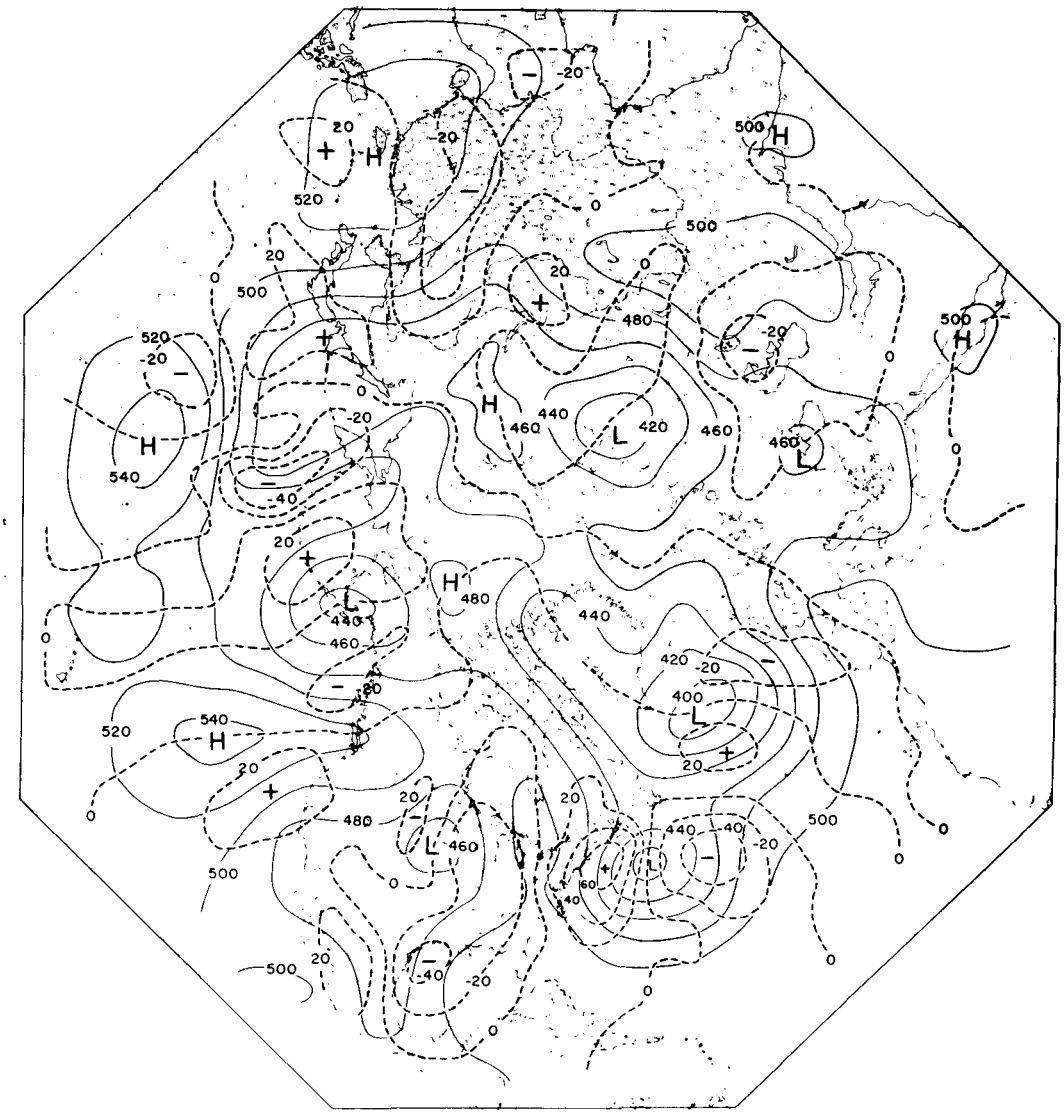

FIGURE 5.—0300 GMT, April 5, 1955. 850-mb. stream function (solid lines) obtained through the balance equation. Superimposed (dashed lines) is the horizontal velocity divergence computed by means of a simple prediction model [7]. Units 10^{-7} sec.$^{-1}$

where A is the computed stream function and B, the forecast value. There appeared to be no significant difference in either the "pillow" or the root-mean-square error in the cases studied. Table 6 shows the results of six forecasts, and figures 6 and 7 illustrate a typical case. The error fields show marked similarity in the regions of errors greater than 200 feet. It is tentatively concluded that both methods will produce stream functions which essentially lead to the same barotropic 500-mb. forecasts as obtained by using the balance equation. However, since method I converges more rapidly than method II, particularly in areas of large cyclonic vorticity, the former appears preferable.

A final remark concerns the feasibility of obtaining the predicted geopotential field at the end of a forecast period, assuming this parameter is specifically desired. Since prediction is made with a stream function representing the non-divergent part of the original calculated wind field and the end product is a similar stream function, the final total wind field is unavailable. Hence the inverse problem to the solution of equation (2) for the wind field, namely, the recovery of the geopotential field from the corresponding wind field is not strictly solvable at the end of the prediction period. However, the predicted stream function could be used to obtain the non-divergent part of the wind, and this in turn

TABLE 6.—*Results of 24- and 48-hour forecasts*

Method used to obtain initial stream function	24-hour barotropic forecasts		48-hour barotropic forecasts	
	Pillow [1]	RMSE	Pillow [1]	RMSE
Balance equation	(−)23	151	(−)43	226
Method I	(−)25	161	(−)53	241
Method II	(−)24	149	(−)48	221

[1] The numbers here give the average magnitude of the pillow; the sign in parentheses gives most frequent sign.

633645—62——2

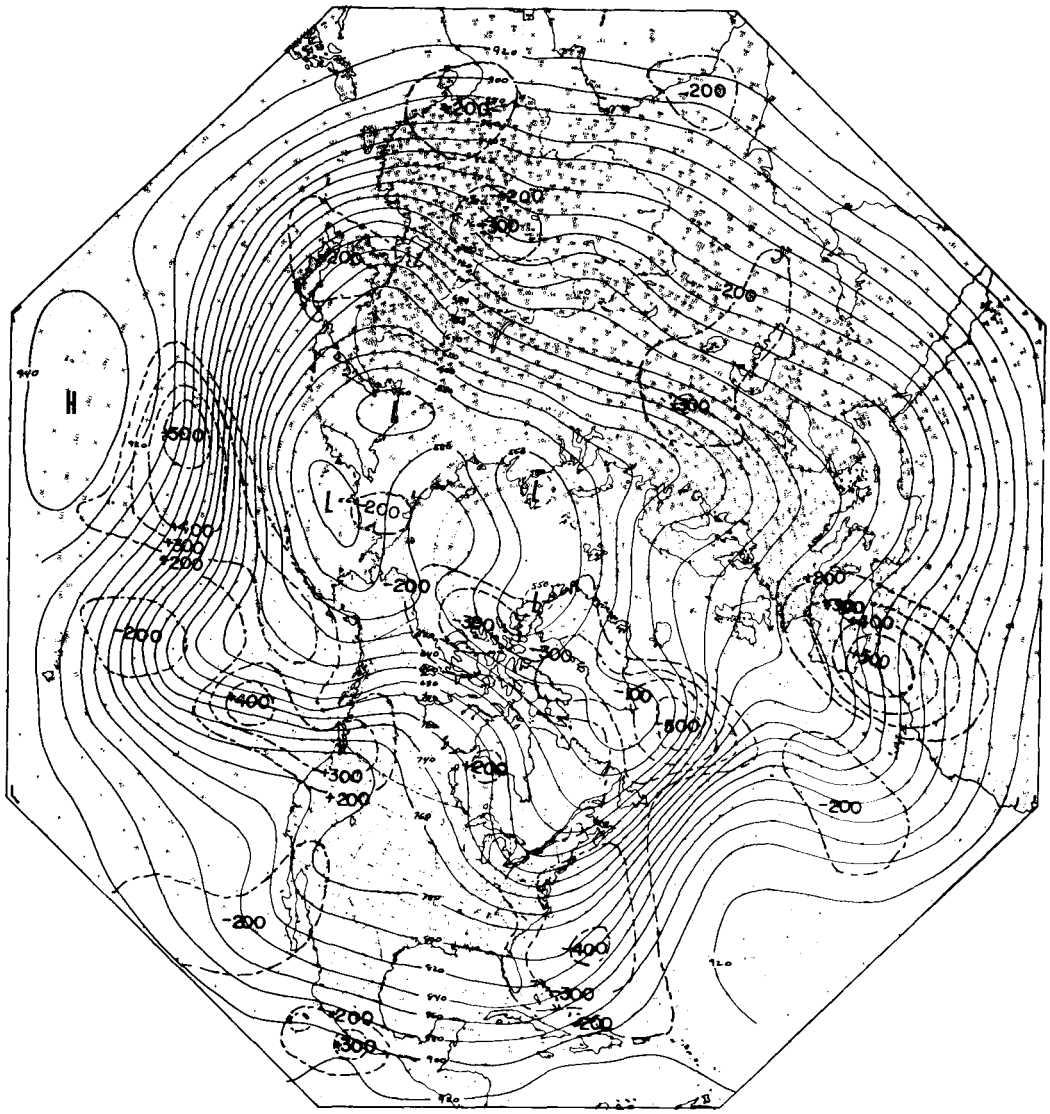

FIGURE 6.—0000 GMT, January 4, 1958. 500-mb. stream function (solid lines) obtained from method I after one iteration. Superimposed (dashed) is the error map of the 24-hr. forecast from 0000 GMT, January 3, 1958.

could be used in equation (2) to determine the geopotential field. This is, of course, equivalent to solving the balance equation for the geopotential field, which is a straightforward relaxation procedure. Since systematic differences were noted between the stream fields computed herein and those obtained from the balance equation, similar differences may be expected in the recovered geopotential fields. However the character of these differences suggests that an empirical correction, which is a function of latitude, might be applied to give a more accurate height field.

5. SUMMARY AND CONCLUSIONS

This paper deals with two methods for obtaining horizontal winds from the pressure-height distribution in an attempt to improve upon the geostrophic wind and avoid solution of the so-called balance equation. Both methods involve computations of higher-order height derivatives, and successive iterations are used for the purpose of a gradual refinement. The convergence properties of both iterative schemes are discussed at some length.

A few barotropic 500-mb. forecasts were made based on stream functions derived from both methods of wind computations and compared with barotropic forecasts using a stream function derived by solving the balance equation. The following conclusions were reached:

a) Wind and vorticity derived by either method are in general intermediate between their geostrophic counterparts and those obtained by means of the balance equation.

b) Successive iteration does not always lead to improved winds. In areas of strong height derivatives combined with negative relative vorticity, both methods may break down in the sense that differences between successive wind approximations become larger with increasing

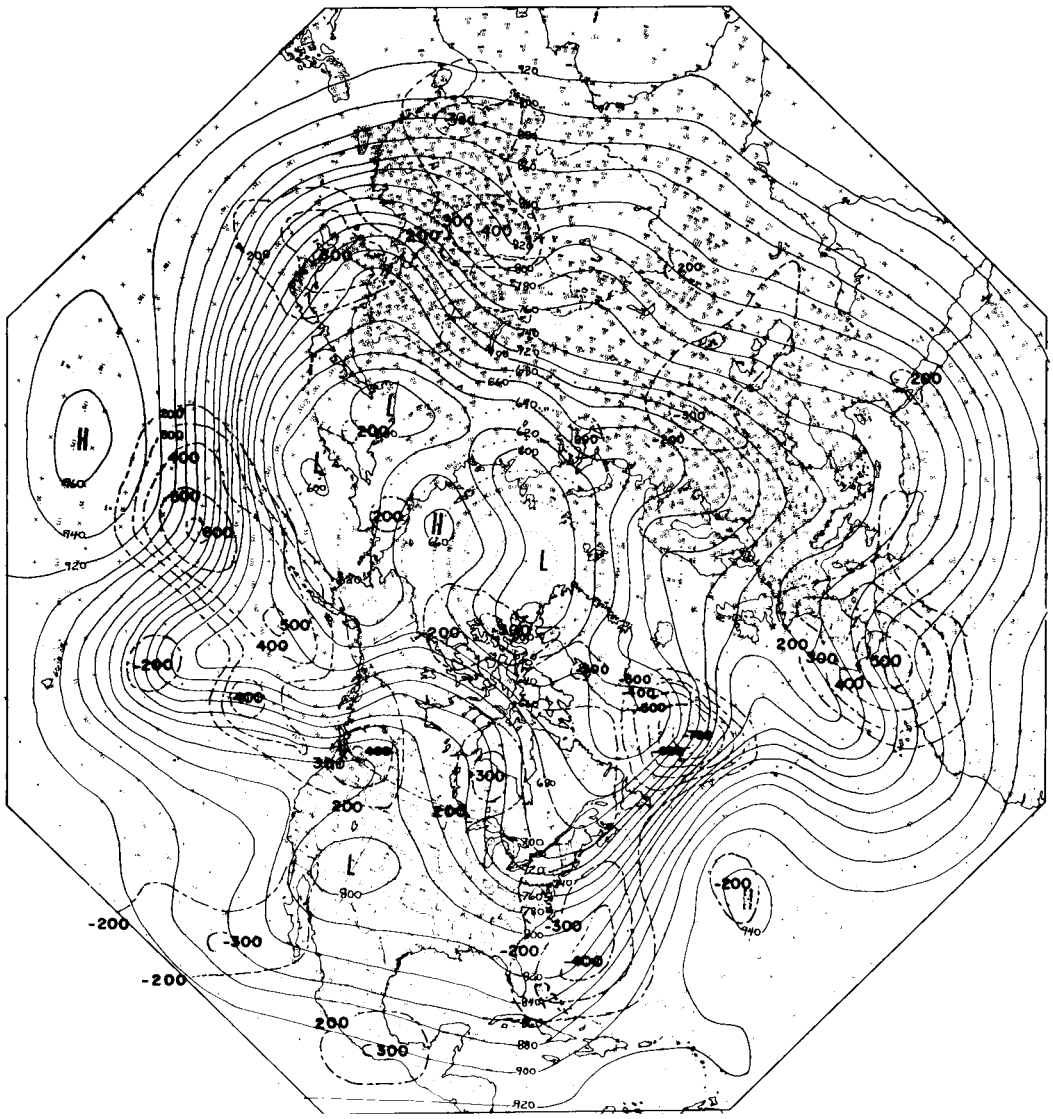

FIGURE 7.—0000 GMT, January 4, 1958. 500-mb. stream function (solid lines) obtained through the balance equation. Superimposed (dashed) is the error map of the 24-hr. forecast from 0000 GMT, January 3, 1958.

number of iterations. This breakdown is accompanied by development of excessive velocity divergence.

c) If one applies one or two iterations only, one of the methods at least results in winds that may be considered a fair substitute for those obtained by the use of the balance equation. This may be of some importance for the time economy of routine operations.

d) Barotropic forecasts using initial wind data computed by either method without iteration are essentially the same as barotropic forecasts with the stream function from the balance equation.

REFERENCES

1. H. Philipps, "Die Abweichung vom Geostrophischen Wind," *Meteorologische Zeitschrift*, vol. 56, 1939, pp. 460–483.
2. A. Eliassen, "The Quasi-Static Equations of Motion with Pressure as Independent Variable," *Geofysiske Publikasjoner*, vol. 17, No. 3, 1949, pp. 1–44.
3. R. M. Endlich, "Computation and Uses of Gradient Winds," *Monthly Weather Review*, vol. 89, No. 6, June 1961, pp. 187–191.
4. G. 'Arnason, "A Convergent Method for Solving the Balance Equation," *Journal of Meteorology*, vol. 15, No. 2, Apr. 1958, pp. 220–225.
5. S. L. Rosenthal, "Concerning the Feasibility of Computing the Field of Pressure-Geopotential from Observed Winds by Use of the Divergence Equation," *Technical Report* No. 15, Department of Meteorology, Florida State University, 1960.
6. G. J. Haltiner and F. L. Martin, *Dynamical and Physical Meteorology*, McGraw-Hill Book Co., Inc., New York, 1957, 470 pp.
7. G. 'Arnason, "A Study of the Dynamics of a Stratified Fluid in Relation to Atmospheric Motions and Physical Weather Prediction," *Tellus*, vol. 13, No. 2, May 1961, pp. 156–170.
8. G. J. Haltiner, "Weather Prognosis by Dynamical Methods," U.S. Naval Postgraduate School, Department of Meteorology (pp. 1–27).
9. G. P. Cressman, "Barotropic Divergence and Very Long Atmospheric Waves," *Monthly Weather Review*, vol. 86, No. 8, Aug. 1958, pp. 293–297.